Hydrol. Earth Syst. Sci. Discuss., 8, 1705–1727, 2011
www.hydrol-earth-syst-sci-discuss.net/8/1705/2011/
doi:10.5194/hessd-8-1705-2011

Hydrology and Earth System Sciences Discussions

Low-frequency variability of European runoff

L. Gudmundsson[1], **L. M. Tallaksen**[1], **K. Stahl**[1,2], **and A. K. Fleig**[1]

[1]Department of Geosciences, University of Oslo, Norway
[2]Institute of Hydrology, University of Freiburg, Germany

Received: 1 February 2011 – Accepted: 2 February 2011 – Published: 7 February 2011

Correspondence to: L. Gudmundsson (lukas.gudmundsson@geo.uio.no)

Published by Copernicus Publications on behalf of the European Geosciences Union.

Abstract

This study investigates the low-frequency components of observed monthly runoff in Europe, to better understand the runoff response to long-term variations in the climate system. The relative variance and the dominant space-time patterns of the low-frequency components of runoff were considered, in order to quantify their relative importance and to get insights in to the controlling factors.

The analysis of a recently updated European data set of observed streamflow and corresponding time series of precipitation and temperature, showed that the fraction of low-frequency variance of runoff is on average larger than, and not correlated to, the fraction of low-frequency variance of precipitation and temperature. However, it is correlated with catchment properties as well as mean climatic conditions. The fraction of low-frequency variance of runoff decreases for catchments that respond more directly to precipitation. Furthermore, it increases (decreases) under drier (wetter) conditions – indicating that the average degree of catchment saturation may be a primary control of low-frequency runoff dynamics.

The dominant space-time patterns of low-frequency runoff, identified using nonlinear dimension reduction, revealed that low-frequency runoff can be described with three modes, explaining together 80.6% of the variance. The dominant mode has opposing centers of simultaneous variations in northern and southern Europe. The secondary mode features a west-east pattern and the third mode has its centre of influence in central Europe. All modes are closely related to the space-time patterns extracted from time series of precipitation and temperature.

In summary, it is shown that the dynamics of low-frequency runoff follows large-scale atmospheric features, whereas the proportion of variance attributed to low-frequency fluctuations is controlled by catchment processes and varies with the mean climatic conditions. The results may have implications for interpreting the impact of changes in temperature and precipitation on river-flow dynamics.

HESSD

8, 1705–1727, 2011

Low-frequency runoff

L. Gudmundsson et al.

1 Introduction

Catchment runoff depends on atmospheric water input (precipitation) and loss (evapotranspiration) as well as on catchment processes, which determine how atmospheric fluctuations are translated into runoff. On short time scales (days, months) a multitude of processes is known to influence runoff generation. Under a changing climate, fluctuations on longer time scales (years, decades) gain increasing importance. On these time scales runoff variability is known to have systematic space-time patterns (e.g. Lins, 1997; Gudmundsson et al., 2010) that are related to large-scale atmospheric drivers (e.g. Barlow et al., 2001; Tootle and Piechota, 2006). However, the variance of annual runoff varies largely among catchments (for a global analysis see McMahon et al., 2007) and is larger than the variance induced by precipitation and evapotranspiration alone (as demonstrated for US streamflow by Sankarasubramanian and Vogel, 2002). This indicates that terrestrial processes influence the magnitude of runoff fluctuations on longer time scales. Various mechanisms such as groundwater processes (e.g. Shun and Duffy, 1999) and channel routing (e.g. Mudelsee, 2007), have been suggested to explain this phenomenon. Other studies have investigated the sensitivity of annual runoff to fluctuations in the forcing as a function of aridity (e.g. Dooge, 1992; Koster and Suarez, 1999; Sankarasubramanian et al., 2000; Milly and Dunne, 2002). Generally, these studies conclude that long-term runoff is more sensitive to precipitation changes in drier climates.

Most hydrological studies focus either on sub-annual (e.g. rainfall-runoff processes) or long-term variability (e.g. linking annual runoff to large-scale atmospheric drivers). However, little is known about the relative importance of long-term variability as compared to annual or sub-annual variability. This study aims at quantifying the contribution of low-frequency variance (variance on time scales larger than one year) to the total variance of runoff and further, to identify controlling factors. Principally, two factors are likely to influence the fraction of low-frequency variance of runoff. On one hand, runoff variability reflects the meteorological forcing, and thus the fraction of low-frequency variance of runoff may be related to the low-frequency variance in precipitation and temperature. On the other hand, catchment processes are known to influence the dynamical properties of runoff and may thus control the contribution of low-frequency variability.

To better understand the different roles of meteorological forcing and terrestrial processes on low-frequency runoff variability, we adopt the idea that hydrological systems can be considered as low-pass filters (e.g. Milly and Wetherald, 2002). The strength of this filtering depends on catchment properties such as topography, hydrogeology, land-cover and climatic conditions. Accordingly, a runoff series Q can be decomposed into a set of additive sub-series,

$$Q = \sum_{f \in F} Q_f \tag{1}$$

where F denotes a set of frequency bands. Each sub-series Q_f, can additionally be characterized by its variance σ_f^2. In this study, the focus is on runoff variability on time scales larger than 12 months ($1/12 > f > 0$ months^{-1}). The corresponding sub-series is denoted as Q_{Long} and the fraction of low-frequency variance of runoff is

$$\Phi_{\mathrm{Q}} = \frac{\sigma^2_{\mathrm{Q_{Long}}}}{\sigma^2_{\mathrm{Q}}} \tag{2}$$

where $\sigma^2_{\mathrm{Q_{Long}}}$ is the variance of Q_{Long} and σ^2_{Q} is the total variance of the runoff-series Q. Any reduction in the high frequency variance (variance on time scales smaller than one year) will increase the fraction of the low-frequency variance Φ_{Q}, whereas the temporal evolution of the corresponding low-frequency component Q_{Long}, will not change. This framework is used to quantify the relative importance of the low-frequency runoff variability as well as to assess the following two hypotheses on its generation:

1. *The fraction of low-frequency variance of runoff Φ_{Q} primarily depends on catchment processes.* This is tested by correlating Φ_{Q} to indicators of catchment

HESSD
8, 1705–1727, 2011

properties, mean climatic conditions, and fractions of low-frequency variance of precipitation (Φ_P) and temperature (Φ_T).

2. *The temporal evolution of Q_{Long} primarily follows the atmospheric forcing.* This is tested by analyzing the dominant space-time patterns of Q_{Long} and comparing them to patterns of low-frequency precipitation (P_{Long}) and temperature (T_{Long}).

2 Data

The study was based on a set of 358 monthly runoff series over the period 1963 to 2000. This unique data set consists of small, near-natural catchments that are not nested (median catchment size: 300 km^2). Most records originate from the European Water Archive[1] (EWA), a database assembled by the Euro-FRIEND program. The EWA was recently updated and complemented by national data from partners in the WATCH project[2] (Stahl et al., 2010, 2008). Mean catchment elevation and slope, estimated from a high resolution digital elevation model, were obtained from the pan-European river and catchment database CCM2 (Catchment Characterisation and Modelling 2; Vogt et al., 2007).

Observed temperature and precipitation series were not available for the catchments, so instead the WATCH forcing data (WFD) were used (Weedon et al., 2010). The WFD provide bias corrected variables, based on the ERA-40 reanalysis (Uppala et al., 2005), on a 0.5 degree grid. For mid-latitudes this is equivalent to a grid-cell size of approximately 2500 km^2. Only grid-cells with one or more runoff stations were used, resulting in a total of 246 grid-cells. In case of more than one runoff station per grid-cell, the area-weighted average of the runoff values was used.

Mean climatic conditions of all grid-cells were characterized by the mean annual temperature ($\bar{T}$), precipitation ($\bar{P}$) and runoff ($\bar{Q}$) (Fig. 1). The fraction of low-frequency

[1] http://grdc.bafg.de/ewa

[2] http://eu-watch.org/

HESSD
8, 1705–1727, 2011

variance of runoff (Φ_Q), precipitation (Φ_P) and temperature (Φ_T) was used to characterize the strength of fluctuations on long time scales.

The ratio of the 25th (low-flows) to the 75th (high-flows) percentile of daily runoff (Q_{25}/Q_{75}) was used to characterise catchment response to precipitation. The notion of percentiles follows the statistical convention (representing cumulative frequencies) and not the hydrological one (representing exceedance frequencies). The ratio Q_{25}/Q_{75} is related to the shape of the flow duration curve (FDC; Vogel and Fennessey, 1994). High values indicate a flat FDC, reflecting the relatively low variability of flows about the median. A low value corresponds to a steep FDC, and is thus a indicator of a flashy flow regime and a high variance of daily runoff (Gustard et al., 1992).

3 Methods

3.1 Extracting low-frequency components

The low-frequency components of runoff (Q_{Long}), temperature (T_{Long}) and precipitation (P_{Long}) were obtained using the STL algorithm (Cleveland et al., 1990; Venables and Ripley, 2002). STL is a computationally efficient filtering technique that decomposes a time series X into

$$X = X_{\mathrm{Long}} + X_{\mathrm{Seas}} + X_{\mathrm{Resid}} \quad (3)$$

where the seasonal (X_{Seas}) and the low-frequency (X_{Long}) components are separated from the residual (X_{Resid}) using locally weighted scatter-plot smoothing (LOESS) with a tricubic weight function. The seasonal component is identified by smoothing the seasonal sub-series (i.e. the series of all Januaries, Februaries, ...), thus allowing for trends in the seasonal pattern. Here the span (time lags) of the LOESS was set to $\lambda_{\mathrm{Seas}} = 10n + 1$, where n is the length of the series. This effectively replaces the smoothing by the mean of each month and guarantees that all low-frequency variability is captured by X_{Long}. After removing the seasonal component, X_{Long} is separated

HESSD
8, 1705–1727, 2011

from X_{Resid} using LOESS. For the identification of X_{Long}, the LOESS parameter was set to $\lambda_{\mathrm{Long}} = 19$, which is the closest odd integer to $(1.5p)/(1-(1.5/\lambda_{\mathrm{Seas}}))$ ($p = 12$ is the periodicity of the seasonal cycle). This choice guarantees minimal spectral leakage from higher frequencies into X_{Long} (Cleveland et al., 1990). To obtain an optimal decomposition this procedure is iterated a few times. The interested reader is referred to Cleveland et al. (1990) for more details. Figure 2 illustrates such a decomposition.

3.2 Correlation analysis with catchment characteristics

Spearman's rank-correlation coefficient ρ (Spearman, 1987), was used to test the relation between catchment topography, mean climatic conditions and climatic variability on the fraction of low-frequency variance of runoff, Φ_{Q}. In contrast to Pearson's linear correlation coefficient, the rank-correlation coefficient ρ is a nonparametric measure that quantifies the strength of general monotonic relations.

3.3 Spatial patterns of simultaneous variations

Dominant spatial patterns of simultaneous variations of geophysical data are commonly identified using principal component analysis (e.g. Storch and Zwiers, 1999). However, the assumption of linearity decreases the power of this method if the underlying manifold is nonlinear, which is common for geophysical data (e.g. Monahan, 2001; Gamez et al., 2004; Mahecha et al., 2010). Therefore, isometric feature mapping (ISOMAP; Tenenbaum et al., 2000) was used to identify spatial patterns of simultaneous variations in Q_{Long}, P_{Long} and T_{Long}.

Let $\mathbf{X}$ be a column matrix of time series with N columns representing locations and T rows representing time steps. The strength of simultaneous variations at two locations can be measured by the so called geodesic or shortest path distance g_{ij}. This concept is well known in geography where the distance between two locations is measured along the curved earth surface. Figure 3 illustrates the difference between the nonlinear geodesic distance and the commonly used Euclidean distance. The points from

HESSD
8, 1705–1727, 2011
Low-frequency runoff
L. Gudmundsson et al.

the center of the spiral have a short Euclidean distance to points from the outer part. ISOMAP is based on estimating the geodesic distances g_{ij}, resulting in the geodesic distance matrix **G**, using the algorithm of Dijkstra (1959). Finally, the geodesic distance matrix **G** is subject to multidimensional scaling (e.g. Borg and Groenen, 2005), which seeks an Euclidean space **Y** that sufficiently describes **G** with few dimensions. The space **Y** is found as the leading eigenvectors of $\tau(\mathbf{G})$ scaled by the square-root of the corresponding non-zero eigenvalues. $\tau(\mathbf{G}) = \frac{1}{2}\mathbf{H}\mathbf{G}^{(2)}\mathbf{H}$ is a double centering operator, where $\mathbf{G}^{(2)}$ is a matrix of squared distances and $\mathbf{H}_{ij} = \delta_{ij} - \frac{1}{N}$ (δ_{ij} is the Kronecker delta). The coordinates of the space **Y** represent the different spatial locations and similar values indicate simultaneous temporal evolution. Thus, maps of the leading dimensions show spatial patterns of simultaneous variations.

ISOMAP has one free parameter, k, the number of nearest neighbours used to estimate the geodesic distance. Following the procedure of Mahecha et al. (2007), $k = 20$ was found to provide the best choice for representing the spatial structure of Q_{Long}, T_{Long} and P_{Long} with a limited number of dominant modes. Geodesic distances were estimated on Euclidean distance matrices of the standardised versions of the low-frequency components to emphasize common temporal evolution.

Similarity in the spatial patterns of simulations variation, as found by ISOMAP of Q_{Long}, P_{Long} and T_{Long}, was quantified using linear Procrustes analysis (e.g. Borg and Groenen, 2005). The scope is to rotate and to reflect a matrix **B** in such a manner that it matches a matrix **A** as close as possible, without altering the relation between the columns of **B**. Here the matrix **A** contains the standardized leading ISOMAP dimensions of Q_{Long} and **B** contains the standardised leading ISOMAP dimensions of P_{Long} or T_{Long}. Linear Procrustes analysis finds such a rotation by solving $\mathbf{A} = \mathbf{TB}$, where the rotation matrix **T** is found to minimize the sum of squared differences. The strength of this fit can be quantified by

$$r^2 = 1 - \frac{2(1 - \text{trace}(\mathbf{W}))}{\text{trace}(\mathbf{W})^2} \quad (4)$$

HESSD
8, 1705–1727, 2011
Low-frequency runoff
L. Gudmundsson et al.

where **W** is a diagonal matrix containing the singular values of $\mathbf{A}^T\mathbf{B}$. r^2 scales between 0 and 1 and its interpretation is equal to Pearson's correlation coefficient. The significance of r^2 is tested using a resampling test (Peres-Neto and Jackson, 2001).

4 Results

4.1 Low-frequency variance

The fractions of low-frequency variance of runoff (Φ_Q), precipitation (Φ_P) and temperature (Φ_T) have large spatial variability (Fig. 4). Φ_Q is on average largest in central Europe and lowest in the Alps and the inland parts of Scandinavia. Comparison with the spatial distributions of mean annual runoff, precipitation and temperature (Fig. 1) shows that the fraction of low-frequency variance of runoff is generally largest in regions where the mean annual runoff and precipitation are low and the mean annual temperature is high. The spatial patterns of Φ_P and Φ_T differ from the spatial distribution of Φ_Q. Φ_P has the highest values in central Europe and Scandinavia, whereas Φ_T has its largest values in southern France and Denmark. On average, the fraction of low-frequency variance is highest for runoff ($0.01 \leq \Phi_Q \leq 0.53$), followed by precipitation ($0.03 \leq \Phi_P \leq 0.13$) and lowest for temperature ($0.01 \leq \Phi_T \leq 0.04$). The large spread in the fraction of low-frequency variance of runoff, suggests that catchments vary significantly in their sensitivity to long-term climatic fluctuations. Note that the distribution of Φ_Q is extremely skewed. All but nine out of 246 grid-cells have $\Phi_Q \leq 0.3$ indicating that Q_{Long} accounts, in most of the cases, for less than one third of the total runoff variance.

Table 1 summarizes the results of the correlation analysis relating Φ_Q to catchment and climatic properties. Catchment properties are in this study represented by topographic indices (elevation and slope) as well as by the ratio Q_{25}/Q_{75}, characterising catchment response. Φ_Q is neither correlated ($p < 0.01$) with the fraction of low-frequency variance of precipitation (Φ_P) nor with temperature (Φ_T), as also suggested

HESSD
8, 1705–1727, 2011

when comparing their spatial patterns (Fig. 4). This indicates that the fraction of low-frequency variance of the meteorological forcing only has a minor influence on the fraction of low-frequency variance of runoff. The relatively high correlation of Φ_Q with the mean climatic conditions contrasts the minor influence of Φ_P and Φ_T. Negative correlations are found with mean annual precipitation ($\rho = -0.39$) and runoff ($\rho = -0.69$), whereas a positive correlation is found with mean annual temperature ($\rho = 0.59$). Thus, the fraction of low-frequency variance of runoff increases under drier and warmer conditions. Also the topographic indicators, mean elevation and slope, are negatively correlated with Φ_Q (respectively $\rho = -0.41$ and $\rho = -0.46$). They are also correlated with each other as well as with mean climatic conditions. This interrelation makes it difficult to separate the effects of mean climatic conditions and catchment topography. The ratio Q_{25}/Q_{75} is positively correlated to Φ_Q ($\rho = 0.58$), i.e. the fraction of low-frequency variance of runoff increases for catchments with a flat FDC.

4.2 Space-time patterns

The three leading ISOMAP components of Q_{Long}, P_{Long} and T_{Long} (Fig. 5) explain a large amount of the variance of the input matrices (runoff: 80.6%, precipitation: 80.8%, temperature: 90.3%). The three runoff components are strongly related to the corresponding precipitation components ($r^2 = 0.93$, $p \leq 0.001$, see Eq. (4)) and moderately related to the temperature components ($r^2 = 0.79$, $p \leq 0.001$). All remaining components account for less than 1% of the variance. The first components of runoff ($Q1: 59.4\%$), precipitation ($P1: 57.6\%$) and temperature ($T1: 73.5\%$) have very similar spatial patterns. Their common feature is a pronounced north-south gradient across Europe. For runoff and precipitation the gradient is slightly tilted northwest in Scandinavia. The main feature of the second components of runoff ($Q2: 11.9\%$), precipitation ($P2: 15.4\%$) and temperature ($T2: 15.7\%$) is a west-east gradient. This pattern is also common to all three variables with some departures of the runoff component ($Q2$) in Scandinavia. Furthermore, the third components of runoff ($Q3: 9.3\%$) and precipitation ($P3: 7.9\%$) have similar patterns. Their common feature is a gradient from the center of the spatial

HESSD
8, 1705–1727, 2011
Low-frequency runoff
L. Gudmundsson et al.

domain (around Denmark) toward the north and south. The spatial pattern of the third temperature component ($T3$: 1.1%) is different and does not appear to be related to runoff.

5 Discussion

5.1 Low-frequency variance

The fact that Φ_Q is on average larger than and not correlated to Φ_P and Φ_T (Table 1), supports the hypothesis that the fraction of low-frequency variance of runoff is controlled by catchment processes and does not primarily depend on the fraction of low-frequency variance in the meteorological forcing. Generally, storage processes (e.g. soils, groundwater and lakes) will dampen high frequency variability in the meteorological input depending on the storage capacity. Steeper catchments drain faster and major aquifers are less likely to be present in mountainous terrain. Both slope and elevation are negatively correlated with Φ_Q, suggesting a possible effect on the fraction of low-frequency variance of runoff. However, both measures are correlated to mean precipitation and temperature, making it difficult do distinguish between effects related to topography and mean climatic conditions (discussed later). To better assess the effects of catchment storage it would be desirable to include information on the hydrogeology and lake percentage of each catchment. Unfortunately, no suitable data with the necessary resolution are available at the pan-European scale. The ratio Q_{25}/Q_{75} is related to the slope of the flow duration curve and used here as an index of catchment response. The FDC can theoretically (Botter et al., 2008) and empirically (Gustard et al., 1992) be related to storage properties. Thus, the positive correlation between Φ_Q and Q_{25}/Q_{75} suggests that the fraction of low-frequency variance in runoff increases with storage capacity. (Note however, that Q_{25}/Q_{75} is also significantly correlated to mean runoff and precipitation, making it difficult to clearly distinguish the effects of storage and climatic conditions.)

HESSD
8, 1705–1727, 2011

The fraction of low-frequency variance of runoff is not only controlled to catchment properties, it also depends on the mean climatic conditions. Generally, Φ_Q increases for drier and warmer conditions. In humid environments, catchment storages are often close to being saturated and thus runoff is more likely to respond quickly to precipitation, maintaining more of its high-frequency variance (resulting in a low Φ_Q). Similarly, strong seasonal cycles due to the temporary storage of precipitation as snow may result in a low value of Φ_Q, which is a possible explanation of the low values of Φ_Q with low mean annual temperature (especially in the Alps and Scandinavia).

Further investigations are needed to fully resolve the different roles of catchment properties and mean climatic conditions on the fraction of low-frequency variance of runoff. However, the current lack of large-scale high quality data on catchment properties hinders further investigations, and supplementary approaches based on hydrological modelling would go beyond the scope of this study.

5.2 Space-time patterns

The strong similarity in the spatial patterns of low-frequency runoff, precipitation and temperature (Fig. 5) supports the hypothesis that Q_{Long} primarily follows the main atmospheric drivers. Such large-scale patterns in runoff are often related to the general features of atmospheric oscillation (e.g. Tootle and Piechota, 2006; Barlow et al., 2001; Shorthouse and Arnell, 1997). The large amount of variance explained by the first ISOMAP component shows that the low-frequency variations of European runoff are dominated by opposing centers of simultaneous variations in the north and the south. This north-south pattern may be related to the zonal structure of atmospheric circulation where the south of Europe is influenced by subtropical and the north by arctic weather systems. Similar patterns of precipitation (López-Moreno and Vicente-Serrano, 2008), runoff (Shorthouse and Arnell, 1997, 1999) and peak discharges (Bouwer et al., 2008) have been previously related to the North Atlantic Oscillation. The west-east gradient of the second component may be related to a shift in influences between Atlantic and continental weather systems. Located in the zone of westerly winds, climate in western Europe is strongly influenced by the Atlantic Ocean. With increasing distance from the coast this influence diminishes. Also the third components of runoff and precipitation have similar spatial patterns. Both explain a considerable amount of the variance. The location of the pattern in the center of the spatial domain, indicates that it may be related to the spatial distribution of the observations and thus may be an artifact of the analysis. However, comparable structures have been identified as the leading principal component of the standardized precipitation index on time-scales of 24 months (Bordi et al., 2009).

6 Conclusions

This study aimed at quantifying the contribution of low-frequency variance (time scales larger than one year) to the total variance of monthly European runoff and to get insights into the controlling factors. It was shown that the space-time patterns of low-frequency runoff (Q_{Long}) can be described by a few modes of oscillation that have their direct counterparts in precipitation and temperature. This demonstrated that continental-scale patterns of low-frequency runoff dynamics are directly driven by large-scale climatic variability.

The fraction of low-frequency variance of runoff (Φ_Q) was found to be on average larger than, and not correlated to, the fraction of low-frequency variance of precipitation (Φ_P) and temperature (Φ_T), suggesting that catchment processes amplify low-frequency fluctuations. The large spread of Φ_Q across Europe indicates large differences in the sensitivity of runoff to low-frequency variability in the forcing. Both catchment properties and mean climatic conditions were found to be significantly correlated to the fraction of low-frequency variance of runoff. The results indicate that on continental scales the effect of the mean climatic conditions on low-frequency runoff dynamics play an equal, or possibly even larger role, than catchment properties. In general, the fraction of low-frequency variance of runoff, increases under drier conditions where catchments respond less directly to precipitation input.

The mechanisms underlying these observations need to be explored in more detail. None the less, these findings may be of particular interest for climate change studies. The influence of any climate signal may vary largely between rivers, depending on the long-term water budget. Climatic change, however, may influence the mean water budget, eventually changing Φ_Q. In the case of increasingly wetter conditions, low-frequency runoff variability is likely to decline, simplifying water management on a year to year basis. In the case of increasingly drier conditions, low-frequency runoff variability is likely to increase, eventually decreasing predictability and challenge water management.

Acknowledgements. This research contributes to the European Union (FP6) funded Integrated Project WATCH (Contract No. 036946). The provision of streamflow data by all agencies that contributed data to the EWA and to the WATCH project is gratefully acknowledged.

References

Barlow, M., Nigam, S., and Berbery, E. H.: ENSO, Pacific Decadal Variability, and U.S. Summertime Precipitation, Drought, and Stream Flow, J. Climate, 14, 2105–2128, doi:10.1175/1520-0442(2001)014<2105:EPDVAU>2.0.CO;2, 2001. 1707, 1716

Bordi, I., Fraedrich, K., and Sutera, A.: Observed drought and wetness trends in Europe: an update, Hydrol. Earth Syst. Sci., 13, 1519–1530, doi:10.5194/hess-13-1519-2009, 2009. 1717

Borg, I. and Groenen, P. J. F.: Modern Multidimensional Scaling – Theory and Applications, Springer Series in Statistics, Springer, 2 edn., 2005. 1712

Botter, G., Zanardo, S., Porporato, A., Rodriguez-Iturbe, I., and Rinaldo, A.: Ecohydrological model of flow duration curves and annual minima, Water Resour. Res., 44, W08418, doi:10.1029/2008WR006814, 2008. 1715

Bouwer, L. M., Vermaat, J. E., and Aerts, J. C. J. H.: Regional sensitivities of mean and peak river discharge to climate variability in Europe, J. Geophys. Res., 113, D19103, doi:10.1029/2008JD010301, 2008. 1716

Cleveland, R. B., Cleveland, W. S., Mcrae, J. E., and Terpenning, I.: STL: A Seasonal-Trend Decomposition Procedure Based on Loess, Journal of Official Statistics, 6, 3–73, 1990. 1710, 1711

Dijkstra, E. W.: A note on two problems in connexion with graphs, Numerische Mathematik, 1, 269–271, doi:10.1007/BF01386390, 1959. 1712

Dooge, J. C. I.: Sensitivity of Runoff to Climate Change: A Hortonian Approach, Bulletin of the American Meteorological Society, 73, 2013–2024, doi:10.1175/1520-0477(1992)073<2013:SORTCC>2.0.CO;2, 1992. 1707

Gamez, A. J., Zhou, C. S., Timmermann, A., and Kurths, J.: Nonlinear dimensionality reduction in climate data, Nonlinear Processes In Geophysics, 11, 393–398, 2004. 1711

Gudmundsson, L., Tallaksen, L. M., and Stahl, K.: Spatial cross-correlation patterns of European low, mean and high flows, Hydrol. Process., doi:10.1002/hyp.7807, 2010. 1707

Gustard, A., Bullock, A., and Dixon, J. M.: Low flow estimation in the United Kingdom, Tech. Rep. 108, Institute of Hydrology, http://www.ceh.ac.uk/products/publications/lowflowestimationintheunitedkingdom.html, 1992. 1710, 1715

Koster, R. D. and Suarez, M. J.: A Simple Framework for Examining the Interannual Variability of Land Surface Moisture Fluxes, J. Climate, 12, 1911–1917, doi:10.1175/1520-0442(1999)012<1911:ASFFET>2.0.CO;2, 1999. 1707

Lins, H. F.: Regional streamflow regimes and hydroclimatology of the United States, Water Resour. Res., 33, 1655–1667, doi:10.1029/97WR00615, 1997. 1707

López-Moreno, J. I. and Vicente-Serrano, S. M.: Positive and Negative Phases of the Wintertime North Atlantic Oscillation and Drought Occurrence over Europe: A Multitemporal-Scale Approach, J. Climate, 21, 1220–1243, doi:10.1175/2007JCLI1739.1, 2008. 1716

Mahecha, M. D., Martinez, A., Lischeid, G., and Beck, E.: Nonlinear dimensionality reduction: Alternative ordination approaches for extracting and visualizing biodiversity patterns in tropical montane forest vegetation data, Ecological Informatics, 2, 138–149, doi:10.1016/j.ecoinf.2007.05.002, 2007. 1712

Mahecha, M. D., Fürst, L. M., Gobron, N., and Lange, H.: Identifying multiple spatiotemporal patterns: A refined view on terrestrial photosynthetic activity, Pattern Recognition Letters, 31, 2309–2317, doi:10.1016/j.patrec.2010.06.021, 2010. 1711

McMahon, T. A., Vogel, R. M., Peel, M. C., and Pegram, G. G.: Global streamflows – Part 1: Characteristics of annual streamflows, J. Hydrol., 347, 243–259, doi:10.1016/j.jhydrol.2007.09.002, 2007. 1707

Milly, P. C. D. and Dunne, K. A.: Macroscale water fluxes 2. Water and energy supply control of their interannual variability, Water Resour. Res., 38, 1206, doi:10.1029/2001WR000760, 2002. 1707

Milly, P. C. D. and Wetherald, R. T.: Macroscale water fluxes 3. Effects of land processes on variability of monthly river discharge, Water Resour. Res., 38, 1235, doi:10.1029/2001WR000761, 2002. 1708

Monahan, A. H.: Nonlinear Principal Component Analysis: Tropical Indo-Pacific Sea Surface Temperature and Sea Level Pressure, J. Climate, 14, 219–233, doi:10.1175/1520-0442(2001)013<0219:NPCATI>2.0.CO;2, 2001. 1711

Mudelsee, M.: Long memory of rivers from spatial aggregation, Water Resour. Res., 43, W01202, doi:10.1029/2006WR005721, 2007. 1707

Peres-Neto, P. and Jackson, D.: How well do multivariate data sets match? The advantages of a Procrustean superimposition approach over the Mantel test, Oecologia, 129, 169–178, doi:10.1007/s004420100720, 2001. 1713

Sankarasubramanian, A. and Vogel, R. M.: Annual hydroclimatology of the United States, Water Resour. Res., 38, 1083, doi:10.1029/2001WR000619, 2002. 1707

Sankarasubramanian, A., Vogel, R. M., and Limbrunner, J. F.: Climate Elasticity of Streamflow in the United States, Water Resour. Res., 37, 1771–1781, doi:10.1029/2000WR900330, 2000. 1707

Shorthouse, C. and Arnell, N.: FRIEND97 – Regional Hydrology: Concepts and Models for Sustainable Water Resource Management, vol. 246, chap. Spatial and temporal variability in European river flows and the North Atlantic oscillation, 77–85, The International Association of Hydrological Sciences (IAHS), 1997. 1716

Shorthouse, C. and Arnell, N.: The effects of climatic variability on spatial characteristics of European river flows, Physics and Chemistry of the Earth, Part B: Hydrology, Oceans and Atmosphere, 24, 7–13, doi:10.1016/S1464-1909(98)00003-3, european Water Resources and Climate Changes Processes, 1999. 1716

Shun, T. and Duffy, C. J.: Low-frequency oscillations in precipitation, temperature, and runoff on a west facing mountain front: A hydrogeologic interpretation, Water Resour. Res., 35, 191–201, doi:10.1029/98WR02818, 1999. 1707

Spearman, C.: The Proof and Measurement of Association between Two Things, The American Journal of Psychology, 100, 441–471, 1987. 1711

Stahl, K., Hisdal, H., Tallaksen, L., van Lanen, H., Hannaford, J., and Sauquet, E.: Trends in low flows and streamflow droughts across Europe, Tech. rep., UNESCO, Paris, 2008. 1709

Stahl, K., Hisdal, H., Hannaford, J., Tallaksen, L. M., van Lanen, H. A. J., Sauquet, E., Demuth, S., Fendekova, M., and Jódar, J.: Streamflow trends in Europe: evidence from a dataset of near-natural catchments, Hydrol. Earth Syst. Sci. Discuss., 7, 5769–5804, doi:10.5194/hessd-7-5769-2010, 2010. 1709

Tenenbaum, J. B., de Silva, V., and Langford, J. C.: A global geometric framework for nonlinear dimensionality reduction, Science, 290, 2319–2323, 2000. 1711

Tootle, G. A. and Piechota, T. C.: Relationships between Pacific and Atlantic ocean sea surface temperatures and U.S. streamflow variability, Water Resour. Res., 42, W07411, doi:10.1029/2005WR004184, 2006. 1707, 1716

Uppala, S. M., Kållberg, P. W., Simmons, A. J., Andrae, U., Bechtold, V. D. C., Fiorino, M., Gibson, J. K., Haseler, J., Hernandez, A., Kelly, G. A., Li, X., Onogi, K., Saarinen, S., Sokka, N., Allan, R. P., Andersson, E., Arpe, K., Balmaseda, M. A., Beljaars, A. C. M., Berg, L. V. D., Bidlot, J., Bormann, N., Caires, S., Chevallier, F., Dethof, A., Dragosavac, M., Fisher, M., Fuentes, M., Hagemann, S., Hlm, E., Hoskins, B. J., Isaksen, L., Janssen, P. A. E. M., Jenne, R., Mcnally, A. P., Mahfouf, J.-F., Morcrette, J.-J., Rayner, N. A., Saunders, R. W., Simon, P., Sterl, A., Trenberth, K. E., Untch, A., Vasiljevic, D., Viterbo, P., and Woollen, J.: The ERA-40 re-analysis, Quarterly Journal of the Royal Meteorological Society, 131, 2961–3012, doi:10.1256/qj.04.176, 2005. 1709

Venables, W. N. and Ripley, B.: Modern Applied Statistics with S, Springer, iSBN 0-387-95457-0, 2002. 1710

Vogel, R. M. and Fennessey, N. M.: Flow-duration. I: New interpretation and confidence intervals, J. Water Resour. Plann. Manage., 120, 458–504, 1994. 1710

Vogt, J., Soille, P., de Jager, A., Rimaviciute, E., and Mehl, W.: A pan-European River and Catchment Database, Tech. Rep. EUR 22920 EN, EC-JRC, Luxembourg, http://ccm.jrc.ec.europa.eu/documents/CCM2-Report_EUR-22920-EN_2007_STD.pdf, 2007. 1709

von Storch, H. and Zwiers, F. W.: Statistical analysis in climate research, Cambridge University Press, Cambridge, UK, 1999. 1711

Weedon, G., Gomes, S., Viterbo, P., sterle, H., Adam, J., Bellouin, N., Boucher, O., and Best, M.: The WATCH forcing data 1958-2001: a meteorological forcing dataset for land surface- and hydrological-models, WATCH Technical Report 22, (available at www.eu-watch.org), 2010. 1709

Table 1. Spearman's rank correlation coefficients (ρ) between the following set of variables: Fraction of low-frequency variance of runoff (Φ_Q), precipitation (Φ_P) and temperature (Φ_T); mean annual runoff ($\bar{Q}$), precipitation ($\bar{P}$) and temperature $\bar{T}$; the ratio of 25th and 75th percentile of daily runoff $\frac{Q_{25}}{Q_{75}}$; as well as mean catchment elevation (Elev.) and slope. Asterisks (*) indicate significance of the correlations ($p < 0.01$).

		Φ_Q	Φ_P	Φ_T	$\bar{Q}$	$\bar{P}$	$\bar{T}$	Elev.	Slope	$\frac{Q_{25}}{Q_{75}}$
Fraction	Φ_Q	1.00*								
low-freq.	Φ_P	0.11	1.00*							
variance	Φ_T	0.11	0.34*	1.00*						
Mean	$\bar{Q}$	−0.69*	−0.03	−0.19*	1.00*					
climatic	$\bar{P}$	−0.39*	0.02	−0.24*	0.80*	1.00*				
conditions	$\bar{T}$	0.59*	0.00	0.19*	−0.44*	−0.20*	1.00*			
	Elev.	−0.41*	−0.33*	−0.42*	0.51*	0.43*	−0.24*	1.00*		
Topography	Slope	−0.46*	−0.13	−0.45*	0.72*	0.64*	−0.33*	0.76*	1.00*	
Runoff response	$\frac{Q_{25}}{Q_{75}}$	0.58*	−0.23*	−0.21*	−0.31*	−0.15	0.17*	−0.06	−0.11	1.00*

HESSD
8, 1705–1727, 2011
Low-frequency runoff
L. Gudmundsson et al.

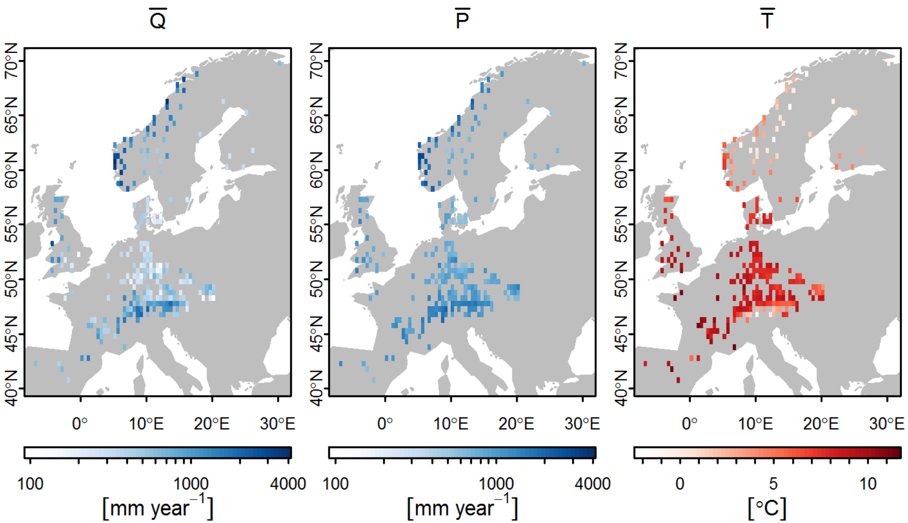

Fig. 1. Mean annual runoff ($\bar{Q}$), precipitation ($\bar{P}$) and temperature ($\bar{T}$) for the period 1962–2000.

HESSD
8, 1705–1727, 2011

Title Page
Abstract | Introduction
Conclusions | References
Tables | Figures
◀| |▶
◀ ▶
Back | Close
Full Screen / Esc
Printer-friendly Version
Interactive Discussion

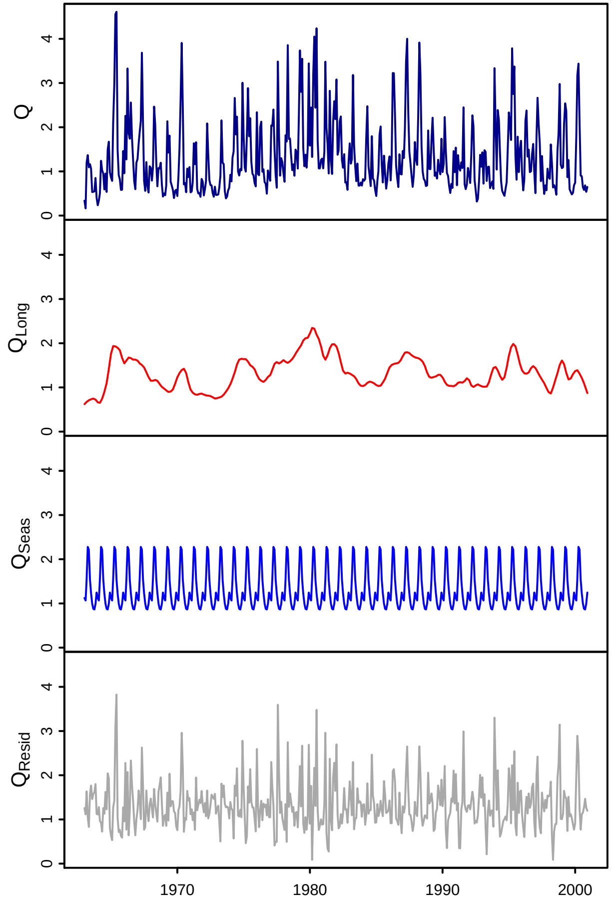

Fig. 2. Decomposition of a monthly runoff series $Q\,[\mathrm{mm}\,d^{-1}]$ into low-frequency (Q_{Long}), seasonal (Q_{Seas}) and residual (Q_{Resid}) components. For visualisation purposes the series mean was added to Q_{Seas} and Q_{Resid}.

HESSD
8, 1705–1727, 2011

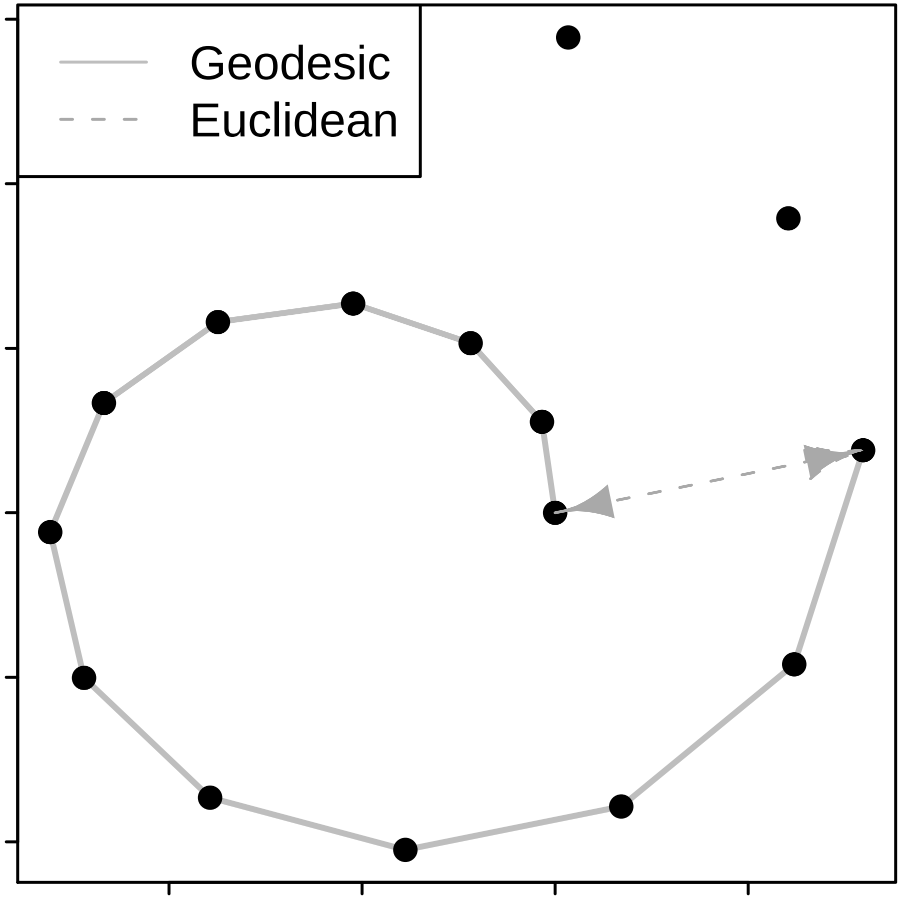

Fig. 3. Illustration on how ISOMAP estimates Geodesic distances as a path of locally linear distances (solid line). The dashed arrow shows the Euclidean distance, which underestimates the difference between data points arising from a nonlinear process.

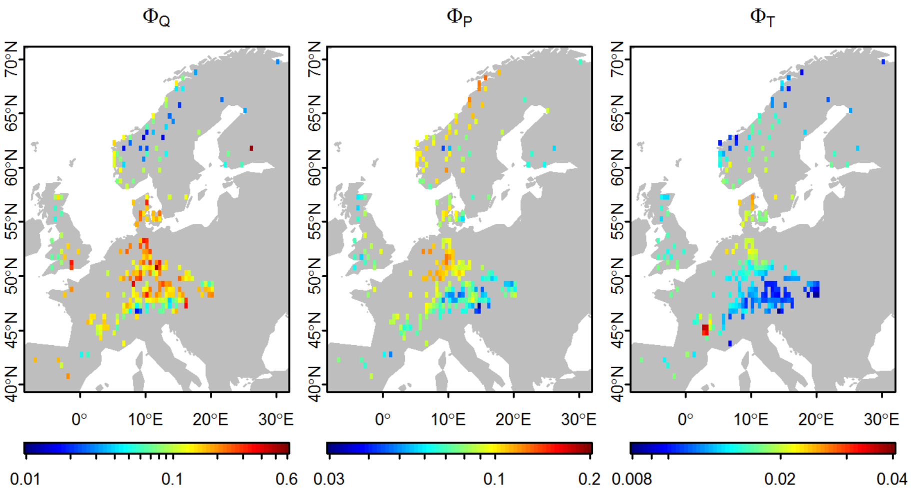

Fig. 4. Spatial pattern of the fraction of low-frequency variance of runoff (Φ_Q), precipitation (Φ_P) and temperature (Φ_P). (Note that each panel has its own logarithmic color scale).

HESSD
8, 1705–1727, 2011

Low-frequency runoff

L. Gudmundsson et al.

Title Page
Abstract | Introduction
Conclusions | References
Tables | Figures
◀| |▶
◀ ▶
Back | Close
Full Screen / Esc
Printer-friendly Version
Interactive Discussion

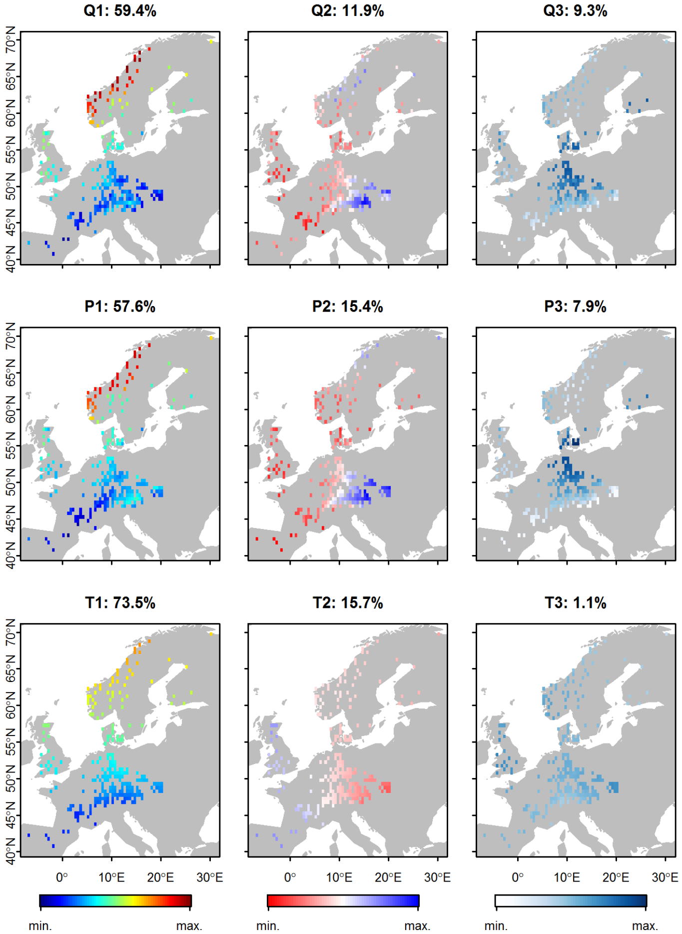

Fig. 5. Spatial patterns of the three dominant modes of low-frequency variability of runoff (Q), precipitation (P) and temperature (T). The numbers in the figure headings are the percentage of explained variance.

HESSD
8, 1705–1727, 2011